Pd(II) AND Pt(II) PINCER COMPLEXES OF A BENZOTHIAZOLE-APPENDED METHYLTHIOACETAMIDE LIGAND: SYNTHESIS AND *IN VITRO* CYTOTOXICITY

Cite this: *INEOS OPEN*, **2021**, *4 (6)*, 237–242
DOI: 10.32931/io2128a

Received 18 March 2022,
Accepted 7 April 2022

http://ineosopen.org

D. V. Aleksanyan,[a]* S. G. Churusova,[a] E. Yu. Rybalkina,[b] Yu. V. Nelyubina,[a] and V. A. Kozlov[a]

[a] *Nesmeyanov Institute of Organoelement Compounds, Russian Academy of Sciences, ul. Vavilova 28, Moscow, 119991 Russia*
[b] *Blokhin National Medical Research Center of Oncology of the Ministry of Health of the Russian Federation, Kashirskoe shosse 23, Moscow, 115478 Russia*

Abstract

The condensation of 2-(benzothiazol-2-yl)aniline with 2-(methylthio)acetyl chloride affords a new representative of non-classical pincer-type ligands based on functionalized amides. This compound is shown to smoothly undergo direct cyclometalation under the action of a Pd(II) or Pt(II) precursor. The realization of the *S,N,N*-coordination in the resulting complexes through the deprotonated central amide unit and ancillary *N*- and *S*-donor groups is unequivocally confirmed by the NMR and IR spectroscopic data as well as X-ray diffraction analysis. The results of comparative cytotoxicity studies of the compounds obtained on several human cancer cell lines are presented.

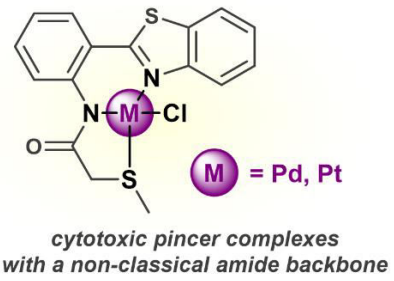

cytotoxic pincer complexes with a non-classical amide backbone

Key words: pincer complexes, functionalized amides, palladium, platinum, cytotoxicity.

Introduction

In search for new potent antitumor agents, significant research efforts have been focused on different transition metal complexes, including the derivatives of ruthenium, gold, copper, rhenium, and, of course, platinum and its closest congener—palladium [1–7]. Among a variety of ligand scaffolds used in the design of new metal-based antitumor agents, recently growing attention has been paid to the so-called pincer-type ligands featuring a specific tridentate monoanionic framework [8]. The latter often combine high tunability with firm coordination of metal ions and thus provide the desired level of control over the system properties, which makes them promising objects for further studies.

Of particular interest are non-classical pincer ligands based on functionalized carboxamides featuring secondary amide central units and ancillary donor groups in the amine and acid parts. They offer such advantages as easy derivatization and propensity for cyclometalation under the action of different transition metals [9–15]. Several series of *N*-metallated Pd(II) and Pt(II) pincer complexes derived from functionalized amides were shown to exhibit prominent cytotoxic activity against different human cancer cell lines (Fig. 1) [16–21]. Our group strategy focused on ensuring the *S,N,N*-hemilabile coordination mainly with incorporation of *S*-donor amino acid residues, which provided the Pd(II) complexes showing considerable cytotoxic effects along with appreciable selectivity towards cancer cell lineages (compounds **I**, Fig. 1) [16, 17]. This approach was equally successful when the methionine residue was initially used as an acid component in the ligand backbone

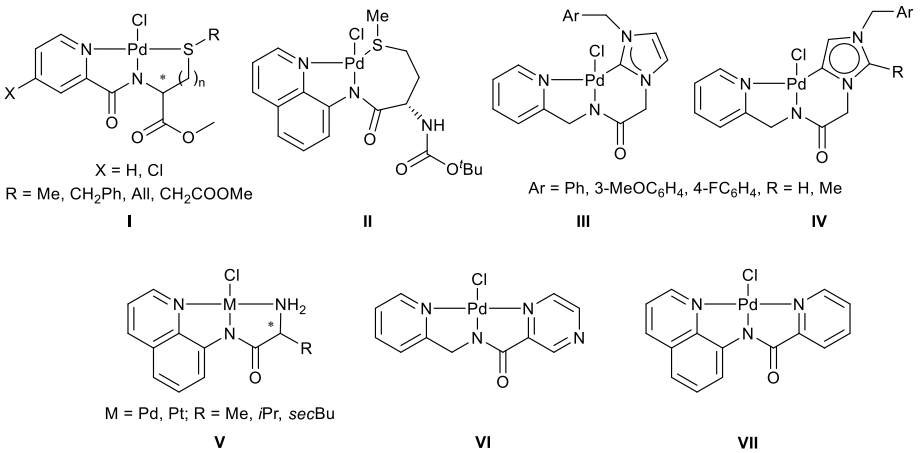

Figure 1. Selected examples of cytotoxic Pd(II) and Pt(II) pincer complexes derived from functionalized amides.

(compound **II**) [18]. The involvement of carbene donor moieties instead of the thioether functionality also afforded some potent palladium(II) candidates (compounds **III** and **IV**) [19]. Another promising way for producing new antitumor agents appeared to be the use of ancillary nitrogen-containing heterocyclic units (for example, compounds **V**–**VII**) [18, 20, 21]. Note that the related Pd(II) and Pt(II) complexes with *N,N,N*-donor sets were found to exhibit also remarkable antibacterial activity [22].

To further explore this line of research, it seemed interesting to combine different design strategies to obtain a new amide-based pincer ligand and make a direct comparison of the cytotoxic properties of its Pd(II) and Pt(II) complexes. The latter is especially interesting since there are only scarce data on the antiproliferative activity of this type of platinum complexes (see, for example, compounds **V** in Fig. 1) and no direct comparison with the analogous Pd(II) derivatives.

Herein, we report on the synthesis and cyclometalation features of a new benzothiazole-appended methylthioacetamide pincer ligand, which contains an *N*-heterocyclic donor moiety and *S,N,N*-donor set. The cytotoxic properties of the resulting Pd(II) and Pt(II) complexes are discussed.

Results and discussion

The desired ligand was obtained upon treatment of 2-(benzothiazol-2-yl)aniline with 2-(methylthio)acetyl chloride in the presence of Et_3N (compound **1**, Scheme 1). The benzothiazolyl ancillary donor moiety was anchored on a carboxamide core through an additional phenylene unit in order to enhance its binding ability with a potential biological target (*e.g.*, DNA) through stacking interactions. Methylthioacetic acid was used as an alternative to the *S*-donor amino acids to enable the hemilabile *S,N,N*-coordination of metal ions. The identity of compound **1** was confirmed by the NMR and IR spectroscopic data, as well as elemental analysis (see the Experimental section and Figs. S1, S2 in the Electronic supplementary information (ESI)).

The direct cyclopalladation of ligand **1** was smoothly accomplished upon interaction with $PdCl_2(NCPh)_2$ in dichloromethane in the presence of Et_3N at room temperature (Scheme 1). Triethylamine was used to trap HCl resulting from the N–H bond metalation to avoid its potential adverse effect (for example, ligand deactivation). The TLC monitoring of the reaction course showed that it was completed already in 0.5 h. Palladium(II) pincer complex **2** was readily isolated after the chromatographic purification in good yield. Unfortunately, the analogous reaction of **1** with $PtCl_2(NCPh)_2$ under mild conditions did not lead to its cyclometalation. However, prolonged heating of the reactants in MeCN afforded the desired pincer-type product (Scheme 1). The moderate yield of complex **3** is likely to be associated with the concomitant formation of some non-metalated species (the latter was deduced from the presence of the free NH amide proton signals in the ^{1}H NMR spectrum of the reaction mixture). Nevertheless, the chromatographic purification afforded the Pt(II) pincer complex of benzothiazole-appended ligand **1** in a pure form.

The structures of complexes **2** and **3** were unambiguously corroborated by the conventional spectroscopic techniques (NMR and IR spectroscopy) and X-ray crystallography. Their compositions were supported by elemental analyses. The occurrence of metalation was confirmed by the absence of characteristic NH stretching and C(O)NH bending vibrations in the IR spectra of the resulting complexes. This was accompanied by a strong low-frequency shift of the C=O stretches from 1665 cm^{-1} for free ligand **1** to 1629 and 1636 cm^{-1} for its cyclometalated derivatives **2** and **3**, respectively. The ^{1}H NMR spectra of the complexes also lacked the downfield signals of the NH protons. Note that the coordination of the deprotonated amide unit through the nitrogen atom led to strong downfield shifts of the adjacent phenylene (C1, $\Delta\delta_C$ = 4.9–5.0 ppm) and carbonyl ($\Delta\delta_C$ > 6.8 ppm) *ipso*-C signals in the ^{13}C NMR spectra. The binding of the thioether coordination arm was evident from the considerable downfield shifts of the signals of carbon and hydrogen nuclei corresponding to the *exo* methyl ($\Delta\delta_C$ ~ 5.5 ppm, $\Delta\delta_H$ ~ 0.35 ppm) and *endo* methylene ($\Delta\delta_C$ > 3.8 ppm, $\Delta\delta_H$ up to 0.62 ppm) groups. Furthermore, the presence of the configurationally stabilized *S*-donor center made the CH_2 protons distinguishable, which was reflected in the splitting of their signal into two strongly deshielded doublets. Finally, a significant upfield shift of the fusion C nucleus attached to the nitrogen atom (C8, $\Delta\delta_C$ = 2.1–2.5 ppm) indirectly confirmed the *N*-coordination of the benzothiazole moiety. Figures S3–S6 in the ESI show the NMR spectra for the complexes obtained.

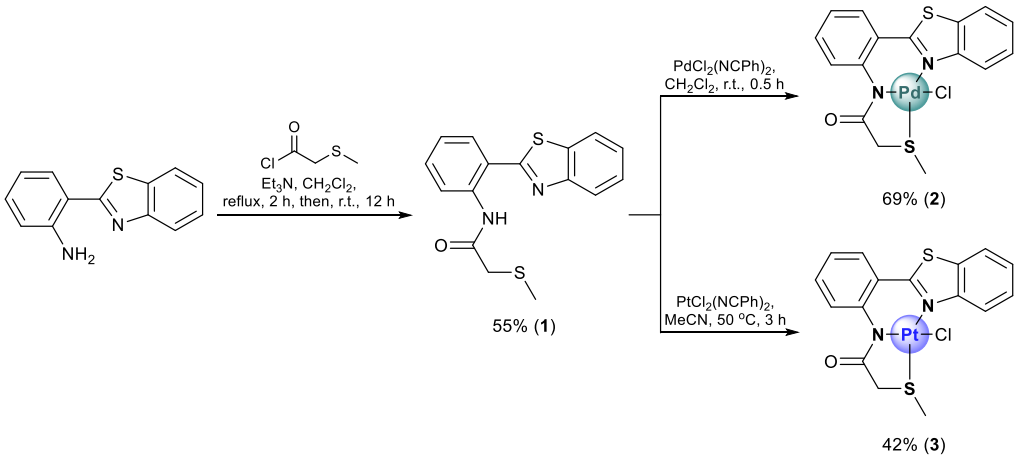

Scheme 1. Synthesis of the benzothiazole-appended methylthioacetamide ligand and its cyclometalated complexes.

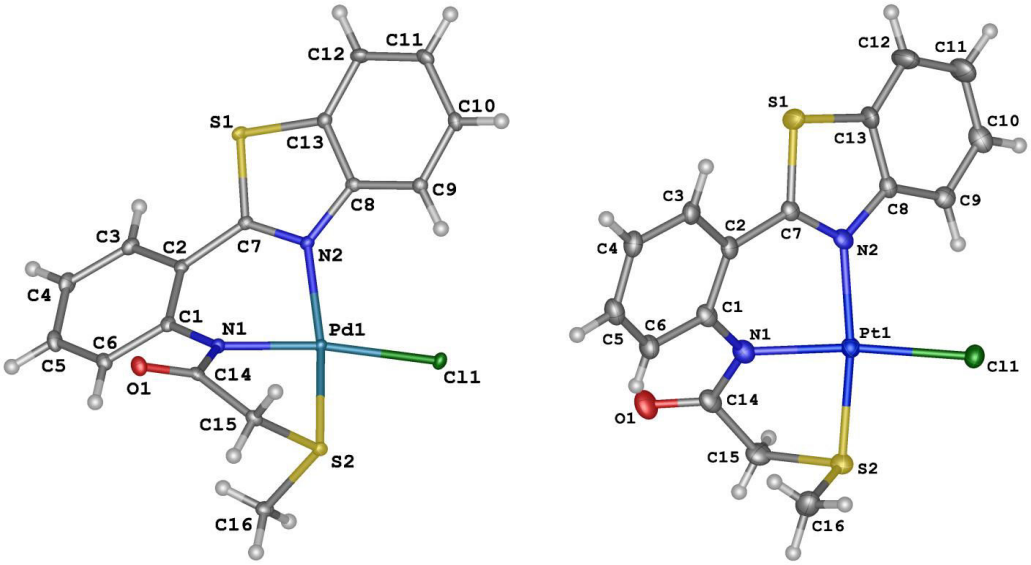

Figure 2. General view of complexes **2** (left) and **3** (right) in representation of atoms *via* thermal ellipsoids at 50% probability level.

The coordination of the ancillary heterocyclic unit through the nitrogen atom was clearly evidenced by the X-ray diffraction analysis (Fig. 2). According to its results, both of the complexes feature distorted square-planar geometry around the metal centers, which is obviously caused by their asymmetric surrounding. This is reflected, in particular, in the wide spread of the *cis*-X–M–Y (X, Y = N, S, or Cl) angles ranging within 82.8–98.5°. Of note is also a remarkable difference in the metal–nitrogen bond lengths reaching up to 0.09 Å in complex **2**. In addition, the slight bends are observed along the N2–Pd1–S2 line in **2** and the N1–Pt1–Cl1 line in **3**. The deviations of S2 (**2**) and Cl1 (**3**) atoms from the mean square planes involving the other coordination sites and metal centers reach 0.410(2) and 0.339(8) Å, respectively. The presence of two fused metallocycles of different sizes additionally contributes to the structural distortions that are less marked in the case of the platinum derivative featuring a larger metal ion. Thus, a six-membered metal-containing ring in **3** adopts a half-chair conformation with the deviation of Pt1 atom by 0.856(3) Å instead of the twisted conformation in its palladium counterpart **2**. Furthermore, C1C2C7N2 dihedral angle between the benzothiazole moiety and the phenylene ring reduces from 28.2(3) to 21.30(11)° on passing from Pd(II) complex **2** to platinum derivative **3**. The main geometric parameters of the complexes explored are summarized in Table 1.

The cytotoxic properties of the compounds obtained were assessed on three cancer cell lines, namely, human colon (HCT116), breast (MCF7), and prostate (PC3) cancer, as well as non-cancerous HEK293 cells derived from a human embryonic kidney. Table 2 lists the half maximal inhibitory concentrations (IC_{50}) defined from the conventional MTT assay. As can be seen, Pd(II) complex **2** was only moderately toxic to HCT116 and PC3 cells. It also exhibited a comparable effect on conditionally normal HEK293 cells. These properties make compound **2** poorly competitive with most of the amino acid-based counterparts with *S,N,N*-donor sets [16, 17] but, at the same time, approach it to the related benzothiazole-substituted monothiooxamide derivative (*i.e.*, another amino-acid free *S,N,N*-palladocycle) [9]. However, the platinum(II) counterpart appeared to be much more cytotoxic against all the cancer lineages explored and provided the IC_{50} rates close to those of cisplatin used as a positive control. Furthermore, complex **3** demonstrated lower cytotoxicity towards HEK293 cell line, with selectivity indices reaching up to 5.4. The latter distinguishes advantageously this compound from the clinically used drug. It is also noteworthy that free ligand **1** did not afford 50% cell growth inhibition even at the concentration of 80 μM, which implies that the observed biological activities of complexes **2** and **3** are mainly determined by the coordination with the metal ions.

Table 1. Selected bond lengths (Å) and angles (°) for complexes **2** and **3**

2			
Pd1–N1	1.9889(17)	N2–Pd1–S2	167.53(5)
Pd1–N2	2.0830(17)	N1–Pd1–N2	87.84(7)
Pd1–S2	2.2608(6)	N2–Pd1–Cl1	98.47(5)
Pd1–Cl1	2.3333(5)	Cl1–Pd1–S2	91.47(2)
N1–Pd1–Cl1	172.58(5)	S2–Pd1–N1	82.81(5)
3			
Pt1–N1	2.014(6)	N2–Pt1–S2	170.38(16)
Pt1–N2	2.058(5)	N1–Pt1–N2	88.1(2)
Pt1–S2	2.2423(19)	N2–Pt1–Cl1	97.72(16)
Pt1–Cl1	2.3367(18)	Cl1–Pt1–S2	90.53(7)
N1–Pt1–Cl1	172.66(17)	S2–Pt1–N1	84.08(18)

Table 2. Cytotoxic properties of the benzothiazole-substituted methylthioacetamide and its cyclometalated derivatives (IC_{50} ± SD, μM)

Compound	Cell lines			
	HCT116	MCF7	PC3	HEK293
1	>80.0[a]	>80.0[a]	>80.0[a]	n/d
2	76.0 ± 8.0	>100	59.5 ± 6.5	64.0 ±5.5
3	14.2 ± 2.8	28.5 ± 2.5	10.0 ± 0.5	54.0 ± 6.0
cisplatin	18.0 ± 2.0	25.0 ± 4.0	16.0 ± 3.0	12.5 ± 1.5

SD is the standard deviation of the value; n/d—not defined;
[a] the percentages of live cells at the compound concentration of 80 μM were as follows: 69% (HCT116), 86% (MCF7), and 68% (PC3).

Conclusions

A new representative of non-classical pincer ligands featuring a central secondary amide unit and ancillary *N*- and *S*-donor groups was synthesized and shown to readily form Pd(II) and Pt(II) complexes. The cytotoxicity studies of the resulting cyclometalated derivatives revealed considerable potential of the Pt(II) complex. Taking into account that a simple molecular architecture of functionalized carboxamide ligands can offer high structural diversity, a search for new potential antitumor agents among their cyclometalated complexes seems to be highly promising.

Experimental

General remarks

If not noted otherwise, all manipulations were carried out without taking precautions to exclude air and moisture. Dichloromethane and acetonitrile were distilled from P_2O_5. Triethylamine was distilled over sodium. 2-(Methylthio)acetyl chloride was synthesized by the reaction of sodium thioglycolate with MeI [23] followed by the treatment of the resulting acid with $SOCl_2$ [24]. 2-(Benzothiazol-2-yl)aniline was obtained from the corresponding nitro derivative according to the published procedure [25]. All other chemicals and solvents were used as purchased.

The NMR spectra were recorded on a Bruker Avance 400 spectrometer, and the chemical shifts (δ) were referenced internally by the residual (^{1}H) or deuterated (^{13}C) solvent signals relative to tetramethylsilane. The $^{13}C\{^1H\}$ NMR spectra were registered using the *J*MODECHO mode; the signals for the C nuclei bearing odd and even numbers of protons had opposite polarities. The NMR peak assignments were made according to the data for the related compounds [9].

The IR spectra were recorded on a Nicolet Magna-IR750 FT spectrometer (resolution 2 cm^{-1}, 128 scans). The assignment of absorption bands in the IR spectra was made according to Ref. [26]. Column chromatography was carried out using Macherey-Nagel silica gel 60 (MN Kieselgel 60, 70–230 mesh). Melting points were determined with an MPA 120 EZ-Melt automated melting point apparatus (Stanford Research Systems).

Syntheses

_N_-[2-(benzo[_d_]thiazol-2-yl)phenyl]-2-(methylthio)acetamide, 1

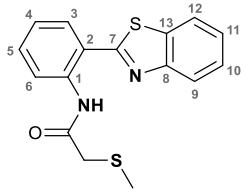

A solution of 2-(methylthio)acetyl chloride (0.44 g, 3.53 mmol) in CH_2Cl_2 (5 mL) was added to a stirred solution of 2-(benzothiazol-2-yl)aniline (0.80 g, 3.53 mmol) and Et_3N (0.50 mL, 3.58 mmol) in CH_2Cl_2 (10 mL). The stirred reaction mixture was refluxed for 2 h and left overnight. The resulting mixture was sequentially washed with water, saturated aqueous solution of $NaHCO_3$, and again with water. The organic layer was separated, dried over anhydrous Na_2SO_4, and evaporated to dryness. The resulting residue was recrystallized from Et_2O–hexane to give 0.61 g of the target compound as yellow crystals. Yield: 55%. Mp: 95–97 °C (Et_2O). ^{1}H NMR (400.13 MHz, $CDCl_3$): δ 2.23 (s, 3H, SMe), 3.53 (s, 2H, CH_2), 7.21–7.24 (m, 1H, H_{Ar}), 7.44–7.57 (m, 3H, H_{Ar}), 7.90 (d, 1H, H_{Ar}, $^3J_{HH}$ = 7.8 Hz), 7.96 (d, 1H, H_{Ar}, $^3J_{HH}$ = 7.8 Hz), 8.12 (d, 1H, H_{Ar}, $^3J_{HH}$ = 8.0 Hz), 8.86 (d, 1H, H_{Ar}, $^3J_{HH}$ = 8.5 Hz), 13.10 (br. s, 1H, NH) ppm. $^{13}C\{^1H\}$ NMR (100.61 MHz, $CDCl_3$): δ 16.35 (s, SMe), 40.13 (s, CH_2), 119.97 (s, C2), 121.15, 121.48, and 122.82 (three s, C6, C9, and C12), 123.64 (s, C4), 125.82 and 126.65 (both s, C10 and C11), 129.93 and 131.87 (both s, C3 and C5), 133.60 (s, C13), 137.64 (s, C1), 153.04 (s, C8), 168.18 and 168.78 (both s, C=O and C7) ppm. IR (KBr, ν/cm^{-1}): 458(w), 494(w), 513(vw), 702(w), 726(m), 738(m), 754(s), 759(s), 793(w), 866(w), 971(m), 1055(w), 1212(m), 1254(m), 1280(m), 1298(m), 1383(w), 1436(m), 1443(m), 1456(m), 1500(s), 1526(s) (C(O)NH), 1582(s), 1607(w), 1665(s) (νC=O in C(O)NH), 2914(w), 3014(w), 3057(w), 3142(vw) (νNH). Anal. Calcd for $C_{16}H_{14}N_2OS_2$: C, 61.12; H, 4.49; N, 8.91. Found: C, 61.24; H, 4.44; N, 8.93%.

Complex [κ^3-*S,N,N*-(L)Pd(II)Cl], 2

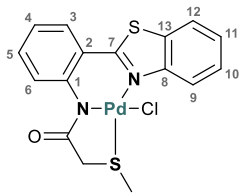

A solution of $PdCl_2(NCPh)_2$ (72 mg, 0.188 mmol) in CH_2Cl_2 (5 mL) was added dropwise to a solution of ligand **1** (59 mg, 0.188 mmol) and Et_3N (27 μL, 0.194 mmol) in CH_2Cl_2 (10 mL). The reaction mixture was left under ambient conditions for 0.5 h and, after TLC control, evaporated to dryness. The resulting residue was purified by column chromatography on silica gel (eluent: first, neat CH_2Cl_2, then CH_2Cl_2/EtOH (5/1)) to give 59 mg of the target pincer complex as a red crystalline solid. Yield: 69%. Mp: >205 °C (dec.). ^{1}H NMR (400.13 MHz, $CDCl_3$): δ 2.59 (s, 3H, SMe), 3.66 (d, 1H, CH_2, $^2J_{HH}$ = 15.9 Hz), 4.12 (d, 1H, CH_2, $^2J_{HH}$ = 15.9 Hz), 7.12–7.16 (m, 1H, H(C4)), 7.44–7.51 (m, 2H, H(C5) + H(C10)), 7.58–7.63 (m, 1H, H(C11)), 7.74 (dd, 1H, H(C3), $^3J_{HH}$ = 7.9 Hz, $^4J_{HH}$ = 1.4 Hz), 7.85 (d, 1H, H(C9), $^3J_{HH}$ = 7.9 Hz), 8.21 (d, 1H, H(C6), $^3J_{HH}$ = 8.6 Hz), 9.28 (d, 1H, H(C12), $^3J_{HH}$ = 8.6 Hz) ppm. $^{13}C\{^1H\}$ NMR (100.61 MHz, $CDCl_3$): δ 21.77 (s, SMe), 44.16 (s, CH_2), 121.45 (s, C9), 123.59 and 124.90 (both s, C4 and C6), 125.32 (s, C2), 125.37, 126.61, and 127.26 (three s, C10, C11, and C12), 130.74 (s, C3), 132.89 (s, C13), 132.99 (s, C5), 142.49 (s, C1), 150.51 (s, C8), 166.87 (s, C7), 175.66 (s, C=O) ppm. IR (KBr, ν/cm^{-1}): 445(vw), 473(vw), 597(vw), 653(vw), 725(vw), 756(m), 990(w), 1165(w), 1227(m), 1272(w), 1307(m), 1324(m), 1426(m), 1444(m), 1457(m), 1479(m), 1563(m), 1594(m), 1629(s) (νC=O in C(O)N), 2914(w), 2965(w), 3078(vw). Anal. Calcd for $C_{16}H_{13}ClN_2OPdS_2$: C, 42.21; H, 2.88; N, 6.15. Found: C, 42.29; H, 2.81; N, 6.11%.

Complex [κ^3-*S,N,N*-(L)Pd(II)Cl], 3

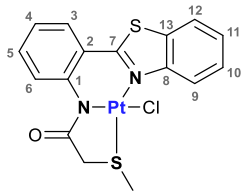

A mixture of $PtCl_2(NCPh)_2$ (33 mg, 0.070 mmol), ligand **1** (22 mg, 0.070 mmol), and Et_3N (10 μL, 0.072 mmol) in MeCN (15 mL) was heated at 50 °C for 3 h. After evaporation to dryness, the resulting residue was purified by column chromatography on silica gel (eluent: CH_2Cl_2/EtOH (100/1)) to give 16 mg of the target pincer complex as a beige crystalline solid. Yield: 42%. Mp: >185 °C (dec.). ^{1}H NMR (400.13 MHz, $CDCl_3$): δ 2.57 (s, 3H, SMe), 3.92 (d, 1H, CH_2, $^2J_{HH}$ = 15.9 Hz), 4.15 (d, 1H, CH_2, $^2J_{HH}$ = 15.9 Hz), 7.09–7.13 (m, 1H, H(C4)), 7.45–7.52 (m, 2H, H(C5) + H(C10)), 7.59–7.63 (m, 1H, H(C11)), 7.79 (d, 1H, H(C3), $^3J_{HH}$ = 8.0 Hz), 7.86 (d, 1H, H(C9), $^3J_{HH}$ = 8.0 Hz), 8.33 (d, 1H, H(C6), $^3J_{HH}$ = 8.5 Hz), 9.30 (d, 1H, H(C12), $^3J_{HH}$ = 8.6 Hz) ppm. ^{13}C{^{1}H} NMR (100.61 MHz, $CDCl_3$): δ 21.95 (s, SMe), 43.93 (s, CH_2), 121.34 (s, C9), 123.63 and 123.67 (both s, C4 and C6), 124.57 (s, C2), 124.97, 126.88, and 127.07 (three s, C10, C11, and C12), 130.38 (s, C3), 132.40 (s, C13), 133.17 (s, C5), 142.68 (s, C1), 150.92 (s, C8), 166.09 (s, C7), 176.53 (s, C=O) ppm. IR (KBr, ν/cm^{-1}): 448(vw), 473(vw), 600(vw), 654(vw), 724(vw), 759(m), 869(vw), 974(vw), 994(w), 1023(vw), 1058(vw), 1168(w), 1226(m), 1244(w), 1272(w), 1324(m), 1425(m), 1444(m), 1457(m), 1481(m), 1565(w), 1594(m), 1636(s) (νC=O in C(O)N), 2915(w), 2968(w), 3078(vw). Anal. Calcd for $C_{16}H_{13}ClN_2OPtS_2$: C, 35.33; H, 2.41; N, 5.15. Found: C, 35.34; H, 2.82; N, 4.89%.

X-ray diffraction

Single crystals suitable for X-ray diffraction analysis were obtained by slow diffusion of hexane into a CH_2Cl_2 (**2**) or $CHCl_3$ (**3**) solution of the compounds explored. The X-ray diffraction data were collected at 120 K with a Bruker APEXII CCD diffractometer using graphite monochromated Mo-K_α radiation (λ= 0.71073 Å, ω-scans). The structures were solved using Intrinsic Phasing with the ShelXT [27] structure solution program in Olex2 [28] and then refined with the XL refinement package [29] using Least-Squares minimization against F^2 in the anisotropic approximation for non-hydrogen atoms. The positions of hydrogen atoms were calculated, and they were refined in the isotropic approximation within the riding model. The crystal data and structure refinement parameters are given in Table 3. CCDC 2158910 and 2158911 contain the supplementary crystallographic data for compounds **2** and **3**, respectively.

Cytotoxicity studies

The cytotoxicities of benzothiazole-substituted methylthioacetamide **1** and its cyclometalated complexes **2**, **3** were studied against human colon (HCT116), breast (MCF7), and prostate (PC3) cancer cell lines as well as non-cancer human embryonic kidney cells (HEK293). All the cell lines were obtained from American Type Culture Collection (ATCC). RPMI-1640 and DMEM media were obtained from Gibco. Fetal bovine serum (FBS) was purchased from HyClone. Cells were cultured in RPMI-1640 (in the case of PC3) or DMEM (in the other cases) media supplemented with 10% FBS and 50 μg/mL gentamicin in a humidified incubator with 5% CO_2 atmosphere. The effect of the compounds on cell viability was estimated using the standard MTT assay (ICN Biomedicals, Germany). Cells were seeded in triplicate at a cell density of 5×103/well in 96-well plates in 100 μL complete medium and preincubated for 24 h. The tested compounds were initially dissolved in DMSO. Then the compounds at various concentrations were added to the media. The well plates were incubated for 48 h followed by addition of MTT solution (Sigma) (20 μL, 5 mg/mL). The cells were incubated at 37 °C for further 3 h; then the culture medium was removed, and formazan crystals were dissolved in DMSO (70 μL). The absorbance of the resulting solutions was measured on a multi-well plate reader (Multiskan FC, Thermo scientific) at 540 nm to determine the percentage of surviving cells. The reported values of IC_{50} are the averages of three independent experiments (Table 2). Cisplatin from a commercial source (in the initial form of an infusion concentrate in natural saline solution) was used as a reference.

Table 3. Crystal data and structure refinement parameters for complexes **2** and **3**

	2	**3**
Empirical formula	$C_{16}H_{13}ClN_2OPdS_2$	$C_{16}H_{13}ClN_2OPtS_2$
Formula weight	455.25	543.94
T, K	120	120
Crystal system	Monoclinic	Orthorhombic
Space group	C2/c	Pbcn
Z	8	8
a, Å	20.3654(15)	18.7916(14)
b, Å	9.5659(7)	9.6694(7)
c, Å	17.3325(13)	18.4584(14)
α, °	90	90
β, °	104.8970(10)	90
γ, °	90	90
V, Å^3	3263.1(4)	3354.0(4)
D_{calc} (g cm^{-1})	1.853	2.154
Linear absorption, μ (cm^{-1})	15.61	87.79
F(000)	1808	2064
$2\theta_{max}$, °	58	54
Reflections measured	31446	32856
Independent reflections	4313	3664
Observed reflections [$I > 2\sigma(I)$]	3776	2660
Parameters	209	209
R1	0.0246	0.0341
wR2	0.0527	0.0822
GOF	1.074	1.068
$\Delta\rho_{max}$/ $\Delta\rho_{min}$ (e Å^{-3})	0.651/–0.401	1.450/–0.974

Acknowledgements

This work was supported by the Russian Science Foundation, project no. 20-73-00282.

The X-ray diffraction data were collected with financial support from the Ministry of Science and Higher Education of the Russian Federation using the equipment of the Center for Molecular Composition Studies of INEOS RAS.

Corresponding author

* E-mail: aleksanyan.diana@ineos.ac.ru (D. V. Aleksanyan)

Electronic supplementary information

Electronic supplementary information (ESI) available online: ^{1}H and ^{13}C{^{1}H} NMR spectra for compounds **1**–**3**. For ESI, see DOI: 10.32931/io2128a

References

1. T. Scattolin, V. A. Voloshkin, F. Visentin, S. P. Nolan, *Cell Rep. Phys. Sci*., **2021**, *2*, 100446. DOI: 10.1016/j.xcrp.2021.100446
2. B. S. Murray, P. J. Dyson, *Curr. Opin. Chem. Biol*., **2020**, *56*, 28–34. DOI: 10.1016/j.cbpa.2019.11.001
3. P. V. Simpson, N. M. Desai, I. Casari, M. Massi, M. Falasca, *Future Med. Chem*., **2019**, *11*, 119–135. DOI: 10.4155/fmc-2018-0248
4. P. Bangde, D. Prajapati, P. Dandekar, I. J. S. Fairlamb, A. R. Kapdi, in: *Palladacycles. Catalysis and Beyond*, A. Kapdi, D. Maiti (Eds.), Elsevier, Amsterdam, **2019**, ch. 9, pp. 343–370. DOI: 10.1016/B978-0-12-815505-9.00010-X
5. T. Lazarević, A. Rilak, Ž. D. Bugarčić, *Eur. J. Med. Chem.*, **2017**, *142*, 8–31. DOI: 10.1016/j.ejmech.2017.04.007
6. P. Zhang, P. J. Sadler, *J. Organomet. Chem.*, **2017**, *839*, 5–14. DOI: 10.1016/j.jorganchem.2017.03.038
7. T. C. Johnstone, K. Suntharalingam, S. J. Lippard, *Chem. Rev*., **2016**, *116*, 3436–3486. DOI: 10.1021/acs.chemrev.5b00597
8. S. Wu, Z. Wu, Q. Ge, X. Zheng, Z. Yang, *Org. Biomol. Chem*., **2021**, *19*, 5254–5273. DOI: 10.1039/D1OB00577D
9. D. V. Aleksanyan, S. G. Churusova, V. V. Brunova, A. S. Peregudov, A. M. Shakhov, E. Yu. Rybalkina, Z. S. Klemenkova, E. G. Kononova, G. L. Denisov, V. A. Kozlov, *Dalton Trans.*, **2021**, *50*, 16726–16738. DOI: 10.1039/d1dt03259c
10. S. Yadav, P. Vijayan, S. Yadav, R. Gupta, *Dalton Trans*., **2021**, *50*, 3269–3279. DOI: 10.1039/d0dt04401f
11. S. S. Kumar, R. S. Kumar, S. K. A. Kumar, *Inorg. Chim. Acta*, **2020**, *502*, 119348. DOI: 10.1016/j.ica.2019.119348
12. L. Mazaud, M. Tricoire, S. Bourcier, M. Cordier, V. Gandon, A. Auffrant, *Organometallics*, **2020**, *39*, 719–728. DOI: 10.1021/acs.organomet.9b00867
13. D. V. Aleksanyan, S. G. Churusova, V. V. Brunova, E. Yu. Rybalkina, O. Yu. Susova, A. S. Peregudov, Z. S. Klemenkova, G. L. Denisov, V. A. Kozlov, *J. Organomet. Chem.*, **2020**, *926*, 121498. DOI: 10.1016/j.jorganchem.2020.121498
14. V. A. Kozlov, S. G. Churusova, E. Yu. Rybalkina, A. S. Peregudov, G. L. Denisov, D. V. Aleksanyan, *INEOS OPEN*, **2019**, *2*, 172–177. DOI: 10.32931/io1923a
15. K. Herasymchuk, J. Huynh, A. J. Lough, L. R. Fernández, R. A. Gossage, *Synthesis*, **2016**, *48*, 2121–2129. DOI: 10.1055/s-0035-1561953
16. S. G. Churusova, D. V. Aleksanyan, E. Yu. Rybalkina, O. Yu. Susova, V. V. Brunova, R. R. Aysin, Y. V. Nelyubina, A. S. Peregudov, E. I. Gutsul, Z. S. Klemenkova, V. A. Kozlov, *Inorg. Chem.*, **2017**, *56*, 9834–9850. DOI: 10.1021/acs.inorgchem.7b01348
17. S. G. Churusova, D. V. Aleksanyan, E. Yu. Rybalkina, O. Yu. Susova, A. S. Peregudov, V. V. Brunova, E. I. Gutsul, Z. S. Klemenkova, Y. V. Nelyubina, V. N. Glushko, V. A. Kozlov, *Inorg. Chem.*, **2021**, *60*, 9880–9898. DOI: 10.1021/acs.inorgchem.1c01138
18. L. Yan, X. Wang, Y. Wang, Y. Zhang, Y. Li, Z. Guo, *J. Inorg. Biochem.*, **2012**, *106*, 46–51. DOI: 10.1016/j.jinorgbio.2011.09.032
19. J.-Y. Lee, J.-Y. Lee, Y.-Y. Chang, C.-H. Hu, N. M. Wang, H. M. Lee, *Organometallics*, **2015**, *34*, 4359–4368. DOI: 10.1021/acs.organomet.5b00586
20. X. Gao, X. Wang, J. Ding, L. Lin, Y. Li, Z. Guo, *Inorg. Chem. Commun*., **2006**, *9*, 722–726. DOI: 10.1016/j.inoche.2006.04.011
21. R. O. Omondi, N. R. S. Sibuyi, A. O. Fadaka, M. Meyer, D. Jaganyi, S. O. Ojwach, *Dalton Trans*., **2021**, *50*, 8127–8143. DOI: 10.1039/d1dt00412c
22. M. Kiani, M. Bagherzadeh, S. Meghdadi, F. Fadaei-Tirani, K. Schenk-Joss, N. Rabiee, *Appl. Organomet. Chem.*, **2020**, *34*, e5531. DOI: 10.1002/aoc.5531
23. Q. Liang, J. Zhang, W. Quan, Y. Sun, X. She, X. Pan, *J. Org. Chem.*, **2007**, *72*, 2694–2697. DOI: 10.1021/jo070159v
24. A. Mooradian, C. J. Cavallito, A. J. Bergman, E. J. Lawson, C. M. Suter, *J. Am. Chem. Soc.*, **1949**, *71*, 3372–3374. DOI: 10.1021/ja01178a030
25. M. F. G. Stevens, D.-F. Shi, A. Castro, *J. Chem. Soc*., *Perkin Trans. 1*, **1996**, 83–93. DOI: 10.1039/P19960000083
26. L. J. Bellamy, *The Infrared Spectra of Complex Molecules*, Wiley, New York, **1975**.
27. G. M. Sheldrick, *Acta Crystallogr. A: Found. Adv*., **2015**, *71*, 3–8. DOI: 10.1107/S2053273314026370
28. O. V. Dolomanov, L. J. Bourhis, R. J. Gildea, J. A. K. Howard, H. Puschmann, *J. Appl. Crystallogr.*, **2009**, *42*, 339–341. DOI: 10.1107/S0021889808042726
29. G. M. Sheldrick, *Acta Crystallogr*., *Sect. A: Found. Crystallogr*., **2008**, *64*, 112−122. DOI: 10.1107/S0108767307043930